REPORT No. 667

DETERMINATION OF THE PROFILE DRAG OF AN AIRPLANE WING IN FLIGHT AT HIGH REYNOLDS NUMBERS

By JOSEPH BICKNELL

SUMMARY

Flight tests were made to determine the profile-drag coefficients of a portion of the original wing surface of an all-metal airplane and of a portion of the wing made aerodynamically smooth and more nearly fair than the original section. The wing section was approximately the N. A. C. A. 2414.5. The tests were carried out over a range of airplane speeds giving a maximum Reynolds Number of 15,000,000. Tests were also carried out to locate the point of transition from laminar to turbulent boundary layer and to determine the velocity distribution along the upper surface of the wing.

The profile-drag coefficients of the original and of the smooth wing portions at a Reynolds Number of 15,000,000 were 0.0102 and 0.0068, respectively; i. e., the surface irregularities on the original wing increased the profile-drag coefficient 50 percent above that of the smooth wing.

INTRODUCTION

Only comparatively recently have profile-drag determinations in the upper range of flight Reynolds Numbers (10,000,000 to 30,000,000) been made, either in wind tunnels or in flight. Profile-drag coefficients up to a Reynolds Number of 13,000,000 have been determined in the 5- by 7-meter tunnel of the DVL (reference 1). In the variable-density tunnel of the N. A. C. A., similar measurements have been made up to an effective Reynolds Number of 8,000,000 (references 2 and 3). An extrapolation equation is suggested in reference 2 for extending the results to higher Reynolds Numbers.

In view of the simplicity of the momentum method of determining profile drag in flight (reference 4), a project was initiated to determine the profile drag of an airplane wing at as high Reynolds Numbers as possible. The project also included measurements to determine the point of transition from laminar to turbulent boundary layer on the upper surface of the wing and the distribution along the wing of the velocity just outside the boundary layer.

APPARATUS AND METHODS

The flight tests were conducted on a Northrop attack airplane (A–17A), a low-wing single-engine monoplane. The tests were carried out on a panel of 5-foot 2-inch span located on the right wing. The inboard edge of this panel was at the juncture of the wing stub and the main wing panel, 5 feet 6 inches from the center line of the airplane. The propeller, 9 feet 9½ inches in diameter, was located 6 feet ahead of the wing leading edge. The test panel was sufficiently removed from the slipstream to avoid interference, especially in the high-speed condition in which the tests were made.

The panel was made smooth by filling the lap joints in the metal-wing covering and then cementing pieces of rubber sheeting to the wing surface in the spaces between the rows of rivets to build up the surface above the level of the rivet heads. The fairness of the wing was improved by cementing a layer of $\frac{1}{32}$-inch-thick hard aluminum to the rubber. This metal was applied in several pieces, rolled to the contour of the wing. Finally, another layer of rubber was applied over the metal. This layer was continuous from the trailing edge around the leading edge and back to the trailing edge, where the two ends were sewed together. The surface of the rubber was sprayed with several coats of filler and was sanded and rubbed until it had a smooth, glossy finish (fig. 1).

On the lower surface of the smooth panel were three small, irremovable obstructions. These obstructions were downstream of the transition point, off to one side of the survey plane, and were faired. The drag and the interference due to these obstructions were estimated on the assumption of a drag coefficient of 1 based on their cross-sectional areas and a reasonable spreading of their wakes. Their estimated effect on the profile-drag coefficient was an increase of 0.0003. This amount has been subtracted from the profile-drag coefficients found by the momentum surveys.

The test panel of the smooth wing tapered in both chord and thickness ratio. The inner section was approximately the N. A. C. A. 2415.5 with a chord of 9.46 feet; the outer section was the N. A. C. A. 2413.5 with a chord of 8.20 feet. The profile in the plane of the wake surveys was approximately the N. A. C. A. 2414.5 section with a chord of 8.86 feet. Measured ordinates of this profile are given in table I, together with the computed ordinates of the N. A. C. A. 2414.5 section.

static tube is mounted so that it can turn about an axis nearly parallel to the wing chord line. (See fig. 1.) On the inboard end of this tube is fastened a short lever, the end of which is held in contact with a single-lobe plate cam by a spring. A ratchet wheel attached to the cam is advanced one tooth at a time by a click. The click is actuated by a bellows expanded hydraulically by the operation of a piston in the cockpit.

The dynamic and the static pressures of the free stream were obtained from a pitot-static tube mounted

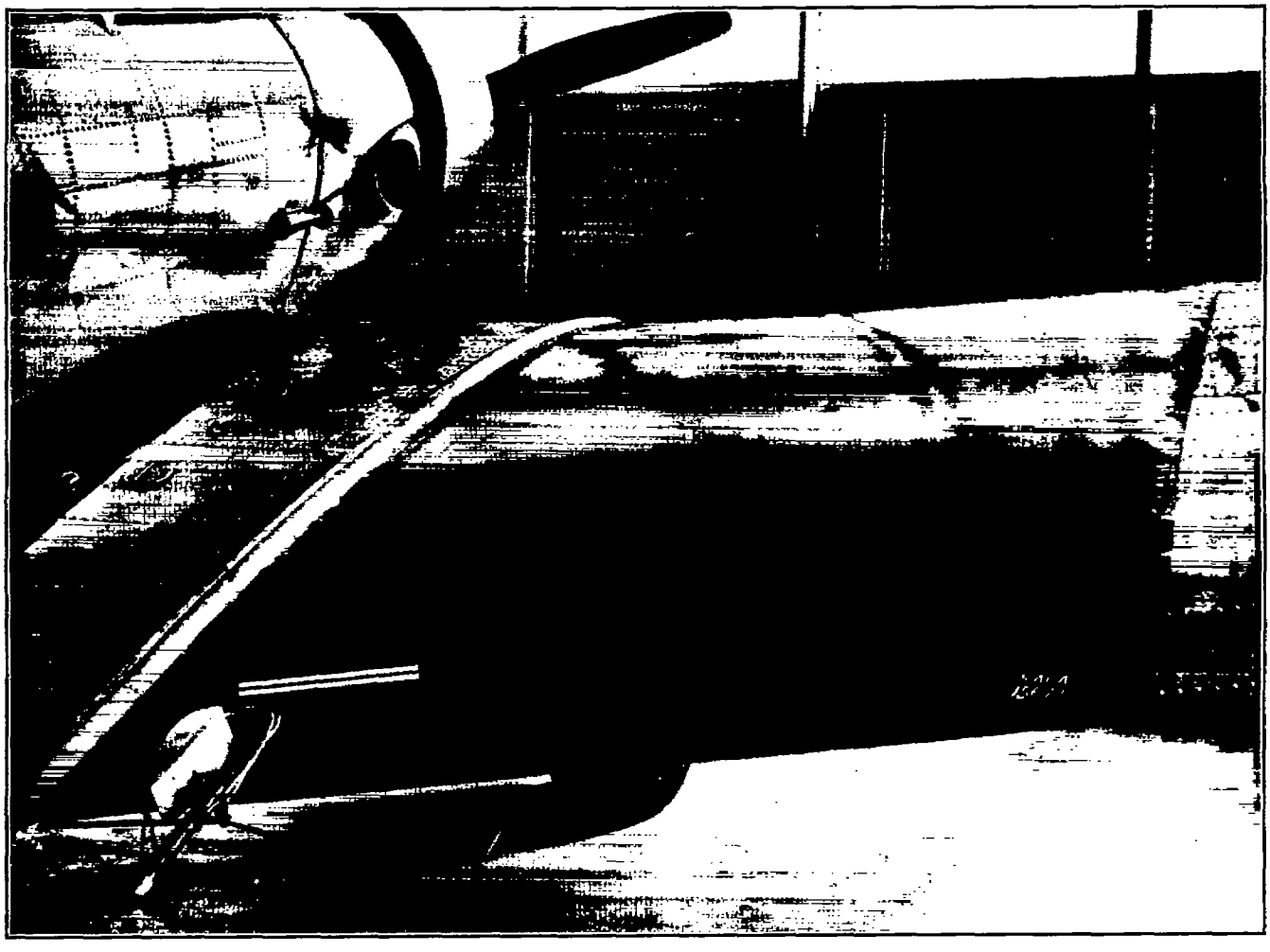

FIGURE 1.—Finished smooth wing and survey apparatus.

The profile drag of the wing with the original surface was determined in the same plane as the smooth wing. The profile was approximately the N. A. C. A. 2414.5 section with a chord of 8.80 feet. Figure 2 shows a photograph of the original wing, and the details of the surface irregularities on this section are given in figure 3.

The profile drag was determined by the momentum method (reference 4). In these tests, the wake surveys were 8.4 percent of the chord behind the trailing edge of the wing. A traversing mechanism to measure, point by point, the total pressure and the static pressure in the wake was developed suitable for attachment to a metal wing. A tube supporting a pitot and a

on a boom near the wing tip. The static tube was calibrated against the static side of a suspended airspeed head.

Measurements to determine the boundary-layer transition point and the pressure distribution were made with three racks mounted on the upper surface, as shown in figure 4. Each rack had a static tube and a total-pressure tube. The static tube was made of 0.040-inch-diameter hypodermic tubing; the total-pressure tube was of the same size flattened at the mouth until its outside depth was 0.012 inch. The static tube was set about $\frac{1}{16}$ inch from the wing surface; the total-pressure tube was in contact with the surface.

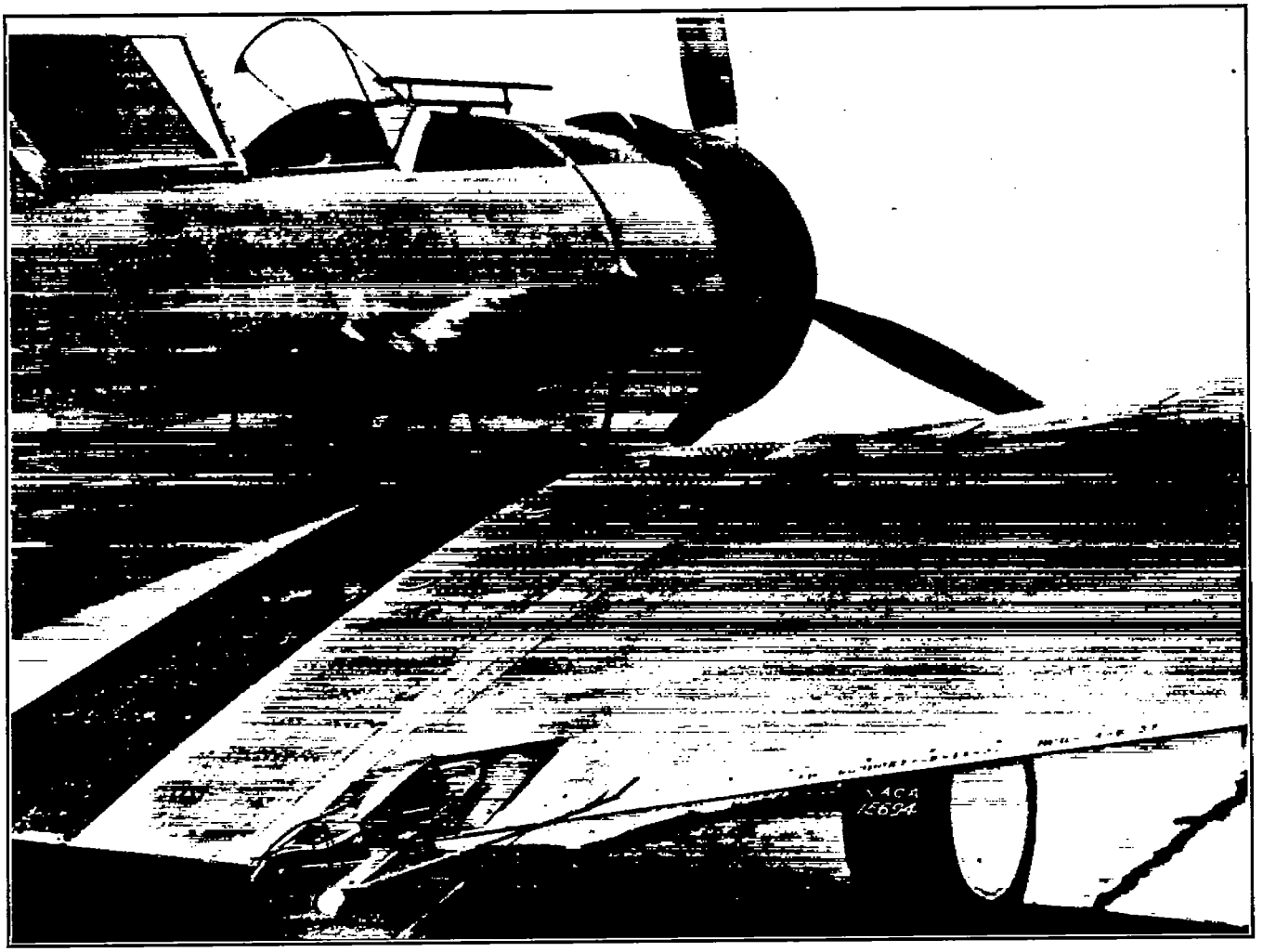

FIGURE 2.—Original wing.

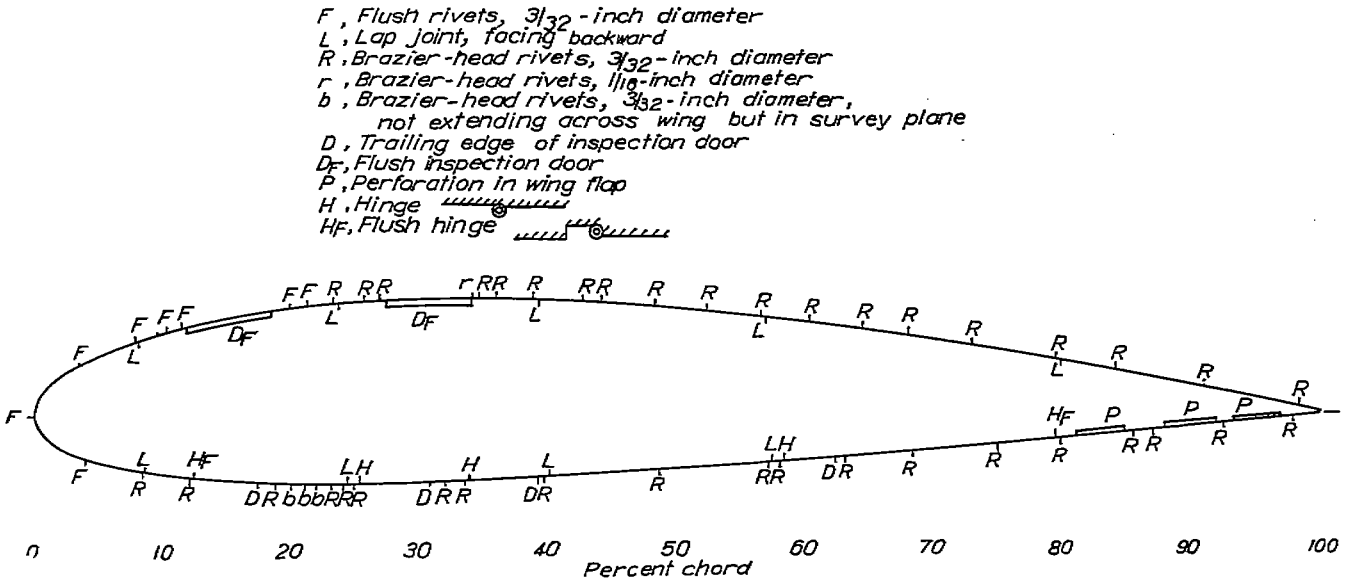

FIGURE 3.—Details of surface irregularities on original wing.

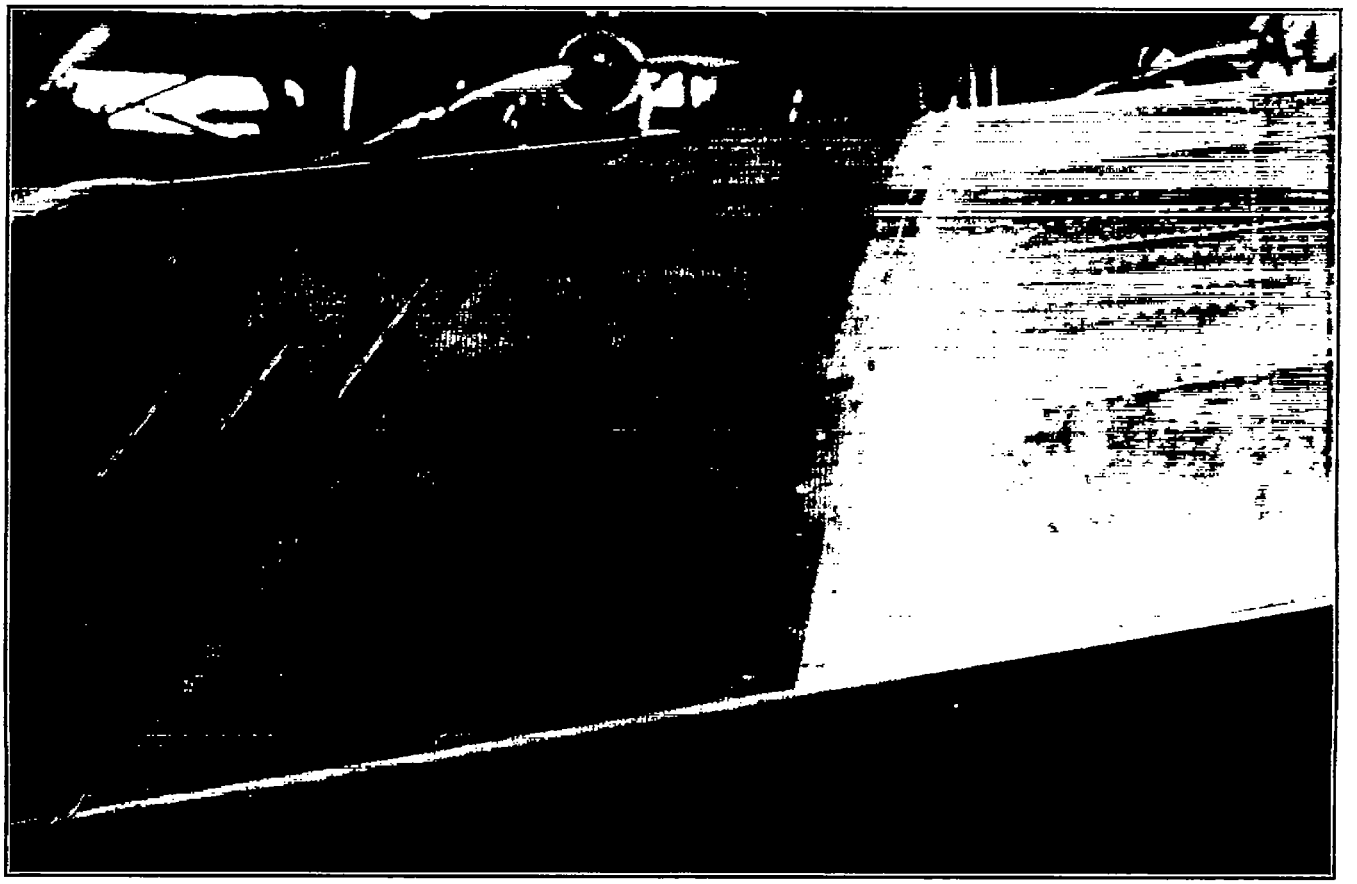

FIGURE 4.—Boundary-layer-tube racks mounted on wing.

The ratio of the dynamic pressure in the boundary layer close to the wing surface to the dynamic pressure just outside the boundary layer was computed and plotted against distance along the surface. The point where this curve shows an abnormal increase in the downstream direction was taken as the transition point from laminar to turbulent boundary layer.

RESULTS AND DISCUSSION

Wake surveys were made over the range of Reynolds Numbers from 11,000,000 to 15,000,000 (air-speed range 140 to 200 miles per hour indicated). The corresponding lift-coefficient range was 0.35 to 0.17. No attempt was made to vary the Reynolds Number R and the lift coefficient C_L independently, since the variation in profile-drag coefficient at constant lift coefficient over the Reynolds Number range that could be obtained in flight was of the same magnitude as that due to experimental errors. The air conditions for these tests ranged from a perfect smoothness to a roughness sufficient to cause small variations in the recorded air speed.

Measurements to determine the boundary-layer transition point on the smooth wing were made at Reynolds Numbers of 11,000,000 and 14,000,000, corresponding to lift coefficients of 0.34 and 0.21, respectively.

Profile-drag coefficients were computed from the wake measurements by Jones' formula (reference 4)

$$c_{d_0}=2\int_W\sqrt{\frac{H_1-p_1}{H_0-p_0}}\left(1-\sqrt{\frac{H_1-p_0}{H_0-p_0}}\right)d\left(\frac{y}{c}\right)$$

where H is total pressure.

p, static pressure.

c, chord.

W, wake.

y, ordinate in survey plane normal to the free stream.

The subscript 0 refers to the free stream at infinity, and the subscript 1 refers to the measurement plane. As a check for possible errors that are a result of assuming the air incompressible, Jones' equation was redeveloped for compressible flow by introducing the equation of continuity and Bernoulli's equation for compressible flow. A complete derivation of the equation is given in the appendix. The final equation is

$$c_{d_0}=2\int_W\left\{\sqrt{\frac{\rho_1}{\rho_0}}-\frac{\sqrt{\frac{H_1-p_1}{F_1}+\left[(p_1-p_0)+\frac{p_1}{2\gamma}\left(\frac{p_1-p_0}{p_1}\right)^2+\cdots\right]}}{\sqrt{\frac{H_0-p_0}{F_0}}}\right\}\times\sqrt{\frac{H_1-p_1}{H_0-p_0}\frac{F_0}{F_1}}d\left(\frac{y}{c}\right)$$

where, in addition to the previously defined symbols,

ρ is density.

γ, ratio of specific heat at constant pressure to specific heat at constant volume.

F, compressibility factor

$$\left[1+\frac{1}{4}(U/V_c)^2+\frac{1}{40}(U/V_c)^4+ \ldots\right]$$

V_c, speed of sound.

U, velocity.

For the position of the survey head 8.4 percent of the chord from the trailing edge of the wing, the correction for compressibility at 200 miles per hour is one-tenth percent of the profile drag. Inasmuch as the static pressure in the wake is nearly equal to free-stream static pressure, the density term is practically unity. The velocity in the wake being a large fraction of the stream velocity, the compressibility factors are approximately equal and cancel out. For the conditions tested, the correction applied to the profile-drag coefficient is negligible.

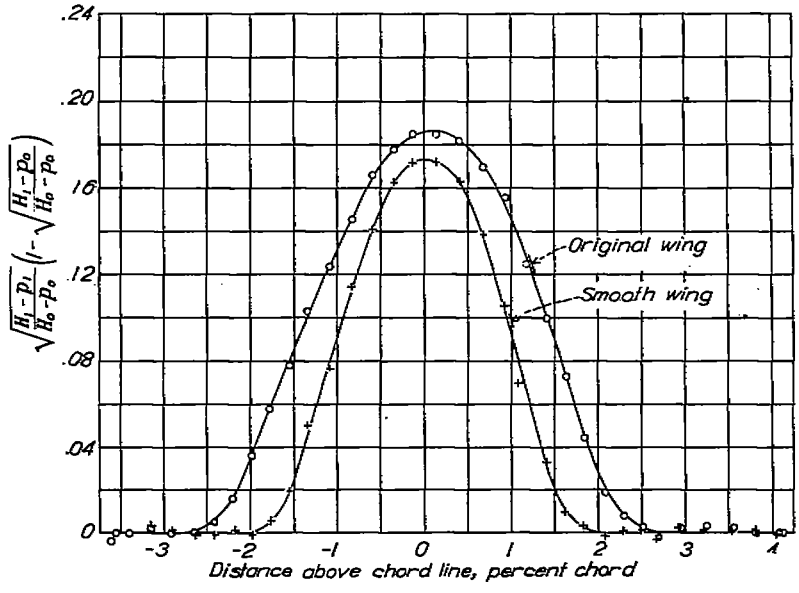

FIGURE 5.—Typical curves of momentum loss in wake. C_L, 0.23.

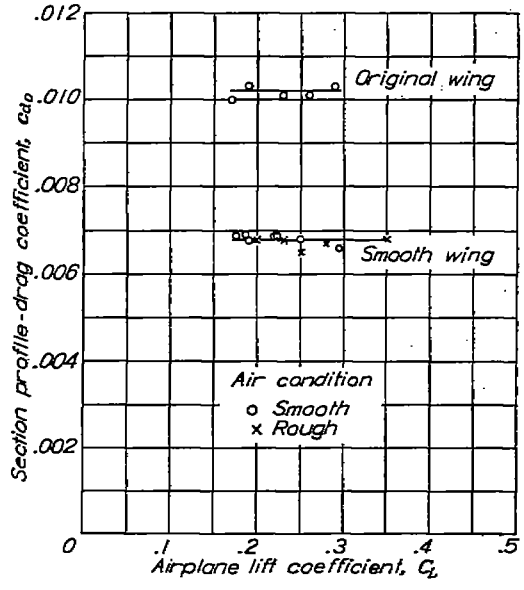

FIGURE 6.—Profile-drag coefficients for smooth and original N. A. C. A. 2414.5 sections.

Typical curves of the momentum loss in the wake for the smooth and the original wing surfaces are given in figure 5. The position of the pitot tube was corrected to its effective center by the method given in reference 5.

The profile-drag coefficients for the smooth condition and the original condition of the wing of N. A. C. A. 2414.5 section are plotted against the lift coefficient of the complete airplane C_L in figure 6. A complete summary of the test conditions and results is given in table II.

The profile-drag coefficient of the smooth wing is 0.0068; of the original wing, 0.0102 for Reynolds Numbers from 12,000,000 to 15,000,000. Thus a profile-drag increase of 50 percent can be attributed to surface irregularities. The original wing had large circular perforations in the wing flap. This construction is not a normal one and undoubtedly accounted for some of the profile drag, although countersunk rivets had been used over the forward 23 percent of the upper surface and 8 percent of the lower surface to keep the drag of the original wing low. Over the range of lift coefficients tested, the profile-drag coefficient is constant within the experimental error and can be taken as $c_{d_{0_{min}}}$. The Reynolds Number range being small, variation of c_{d_0} with Reynolds Number is expected to be very small. From reference 2, the variation of c_{d_0} over the range of lift coefficients tested is also expected to be small.

It is also apparent that c_{d_0} is independent of free-air roughness as no systematic variation was found for different air conditions during the tests. This result has been pointed out by Jones (reference 6). Apparently the type of turbulence found in the atmosphere has no noticeable effect on the profile drag.

From drag data obtained in the variable-density tunnel for the N. A. C. A. 2400 series (reference 3), the interpolated $c_{d_{0_{min}}}$ for the N. A. C. A. 2414.5 section at an effective Reynolds Number of 8,000,000 is 0.0067. If this value is extrapolated to 15,000,000 according to the formula (reference 2),

$$c_{d_{0_{min}}}=\left(c_{d_{0_{min}}}\right)_{8\times10^6}\left(\frac{R}{8\times10^6}\right)^{-0.11}$$

a value of 0.0063 is obtained for $c_{d_{0_{min}}}$.

Profile-drag tests carried out in the 5- by 7-meter tunnel of the DVL on the N. A. C. A. 2409 and 2421 sections over a Reynolds Number range of 3,000,000 to 13,000,000 indicate a $c_{d_{0_{min}}}$ value of 0.0065 for the N. A. C. A. 2414.5 section at a Reynolds Number of 15,000,000.

The $c_{d_{0_{min}}}$ value of 0.0068 for the smooth wing is probably slightly higher than it would have been for a true N. A. C. A. 2414.5 section in flight. This difference can be attributed to earlier transition, as pointed out in the discussion of the boundary-layer tests.

The results of the boundary-layer and the pressure-

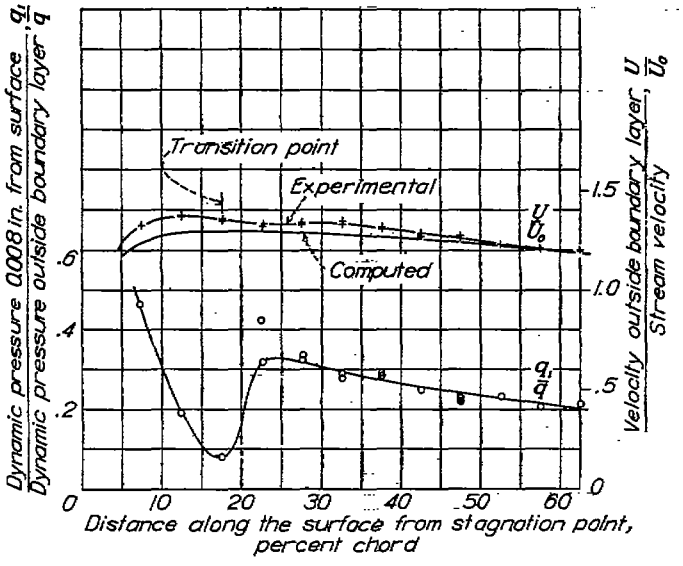

FIGURE 7.—Boundary-layer surveys on upper surface of smooth wing at C_L=0.34. R, 11,100,000; N. A. C. A. 2414.5 section.

distribution surveys are shown in figures 7 and 8 as the velocity distribution along the surface and the ratio of the dynamic pressure q_1 0.008 inch from the surface to the dynamic pressure q just outside the boundary layer.

From the q_1/q curve, the transition point for both flight conditions is 17.5 percent of the chord along the surface from the front stagnation point (14 percent of the chord along the chord line).

For C_L=0.21 (fig. 8), the curve of velocity distribution along the surface reaches a maximum at 14 percent of the chord along the surface. The negative velocity gradient (or positive pressure gradient) exerts thereafter an unstable influence on the laminar boundary layer. Transition to turbulent boundary layer with accompanying increase in skin friction follows soon after the velocity maximum. The tests at C_L=0.34 exhibit the same tendencies.

The dip in the experimental velocity distributions near the quarter-chord point is attributed to departures of the section tested from the true N. A. C. A. 2414.5 section. For comparison, the velocity distributions over the upper surface of a true N. A. C. A. 2414.5 section for the airplane lift coefficients corresponding to those of the boundary-layer tests have been plotted in figures 7 and 8. These distributions were obtained by interpolating between the pressure distributions for the N. A. C. A. 2400 series given in reference 7. Comparison of the experimental and the computed velocity distributions shows that the peak velocity of the computed distributions occurs farther downstream. The transition point would be expected to occur in the region between 25 and 35 percent of the chord measured along the surface. The more forward position of the transition point observed in the tests could easily account for the difference in profile-drag coefficient found in these tests as compared with the DVL and the variable-density-tunnel tests.

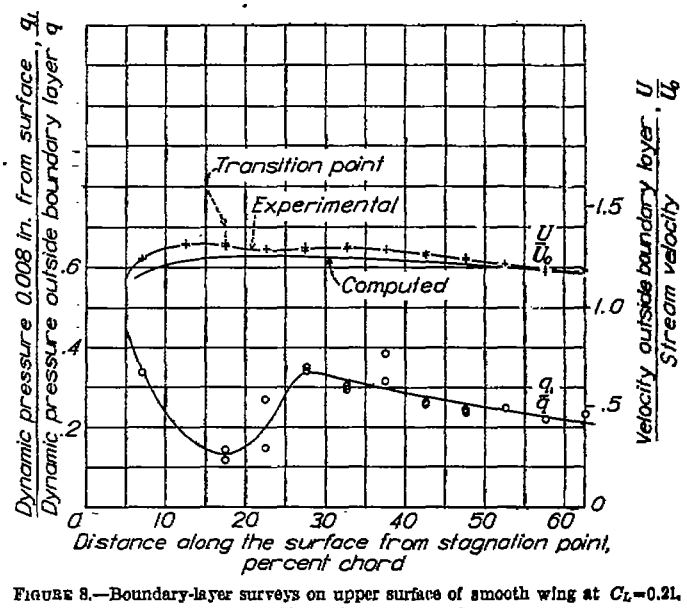

FIGURE 8.—Boundary-layer surveys on upper surface of smooth wing at C_L=0.21. R, 14,000,000; N. A. C. A. 2414.5 section.

CONCLUSIONS

Wake surveys made of a smooth wing of approximately N. A. C. A. 2414.5 section in flight at a Reynolds Number of 15,000,000 gave a minimum profile-drag coefficient of 0.0068. Surveys made of the original wing, which represents current metal construction, gave a profile-drag coefficient of 0.0102. Manufacturing irregularities in rivets, lap joints, access doors, and flap ventilating holes are thus responsible for a 50-percent increase in profile-drag coefficient, even though flush rivets were used over the forward 23 percent of the upper surface and 8 percent of the lower surface of the wing.

The boundary-layer surveys on the upper surface of the smooth wing showed that transition from laminar to turbulent boundary layer occurred at a position on the section tested more forward than would be expected on a true N. A. C. A. 2414.5 section. Differences in the transition-point location could easily account for the slight differences in the profile-drag coefficients of the N. A. C. A. 2414.5 section found in flight and in the DVL and the variable-density tunnels.

The boundary-layer surveys showed that transition occurred a short distance downstream from the point of minimum pressure.

LANGLEY MEMORIAL AERONAUTICAL LABORATORY,
NATIONAL ADVISORY COMMITTEE FOR AERONAUTICS,
LANGLEY FIELD, VA., *January 6, 1939.*

APPENDIX

THE DERIVATION OF JONES' EQUATION FOR PROFILE DRAG IN A COMPRESSIBLE FLUID

Assume a two-dimensional body in a uniform stream (fig. 9). Assume that a plane is located far enough ahead of the body so that the static pressure is equal to the static pressure of the undistributed stream p_0. The velocity, the total pressure, and the density are given as U_0, H_0, and ρ_0, respectively. Assume another plane far enough behind the body so that the static pressure is again the static pressure of the undisturbed stream, p_0. Over an elementary distance dy, normal to the undisturbed stream, the velocity, the total

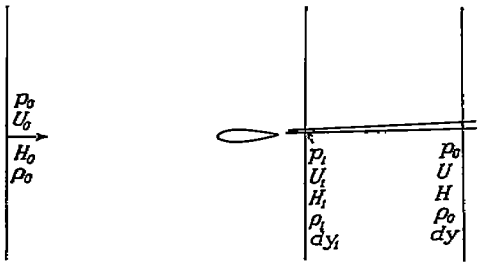

FIGURE 9.

pressure, and the density are given as U, H, and ρ_0, respectively. The density here is equal to ρ_0 since the static pressure is equal to p_0. Over an elementary distance dy_1, to be defined later, of the plane in which the wake surveys are made, the static pressure, the velocity, the total pressure, and the density are p_1, U_1, H_1, and ρ_1, respectively.

Since the static pressures at the forward and the rearward planes are equal, the profile drag per unit span can be equated to the integral of the difference in rate of momentum crossing these planes, namely,

$$D_0=\int_W \rho_0(U_0-U)U\,dy$$

where the integral is taken only over the wake because there is no contribution outside the wake. Assume, as Jones does, that the wake can be considered as made up of "stream tubes" which do not mix as they pass from the measurement plane to the rearward plane and along each of which the total pressure is constant. Then, applying the equation of continuity along the stream tube, whose width is dy_1 at the measurement plane and dy at the downstream plane,

$$\rho_0 U dy=\rho_1 U_1 dy_1$$

Substituting,

$$D_0=\int_W (U_0-U)\rho_1 U_1 dy_1$$

From Bernoulli's equation, in a compressible fluid,

$$H-p=\frac{\rho}{2}U^2\left[1+\frac{1}{4}\left(\frac{U}{V_c}\right)^2+\frac{1}{40}\left(\frac{U}{V_c}\right)^4+\cdots\right]$$

where V_c is the local velocity of sound.

Let

$$F=\left[1+\frac{1}{4}\left(\frac{U}{V_c}\right)^2+\frac{1}{40}\left(\frac{U}{V_c}\right)^4+\cdots\right]$$

Then

$$U_0=\sqrt{\frac{2}{\rho_0}}\sqrt{\frac{H_0-p_0}{F_0}}$$

and

$$U_1=\sqrt{\frac{2}{\rho_1}}\sqrt{\frac{H_1-p_1}{F_1}}$$

Applying Bernoulli's equation for the compressible flow along a stream tube,

$$\frac{U^2}{2}+\frac{\gamma}{\gamma-1}\frac{p_0}{\rho_0}=\frac{U_1^2}{2}+\frac{\gamma}{\gamma-1}\frac{p_1}{\rho_1}$$

where γ is the ratio of the specific heat at constant pressure to the specific heat at constant volume, whence

$$U=\sqrt{\frac{2}{\rho_1}\frac{H_1-p_1}{F_1}+\frac{2\gamma}{\gamma-1}\left(\frac{p_1}{\rho_1}-\frac{p_0}{\rho_0}\right)}$$

Examine now the term

$$\frac{p_1}{\rho_1}-\frac{p_0}{\rho_0}$$

Assuming adiabatic changes of pressure and density,

$$\left(\frac{p_0}{\rho_0}\right)^{1/\gamma}=\left(\frac{p_1}{\rho_1}\right)^{1/\gamma}$$

whence, by substitution,

$$\frac{p_1}{\rho_1}-\frac{p_0}{\rho_0}=\frac{p_1}{\rho_1}\left[1-\left(\frac{p_0}{p_1}\right)^{\frac{\gamma-1}{\gamma}}\right]$$

Now

$$\left(\frac{p_0}{p_1}\right)^{\frac{\gamma-1}{\gamma}}=\left(1+\frac{p_0}{p_1}-1\right)^{\frac{\gamma-1}{\gamma}}=\left(1+\frac{p_0-p_1}{p_1}\right)^{\frac{\gamma-1}{\gamma}}$$

and, expanding this expression by the binomial theorem,

$$\left(\frac{p_0}{p_1}\right)^{\frac{\gamma-1}{\gamma}}=1+\frac{\gamma-1}{\gamma}\frac{p_0-p_1}{p_1}+\frac{\gamma-1}{\gamma}\frac{1}{2\gamma}\left(\frac{p_0-p_1}{p_1}\right)^2+\cdots$$

Substituting

$$\frac{p_1}{\rho_1}-\frac{p_0}{\rho_0}=\frac{1}{\rho_1}\left[\frac{\gamma-1}{\gamma}(p_1-p_0)+\frac{\gamma-1}{2\gamma}\frac{p_1}{\gamma}\left(\frac{p_1-p_0}{p_1}\right)^2+\cdots\right]$$

and, finally,

$$U=\sqrt{\frac{2}{\rho_1}\frac{H_1-p_1}{F_1}+\frac{2}{\rho_1}\left[(p_1-p_0)+\frac{p_1}{2\gamma}\left(\frac{p_1-p_0}{p_1}\right)^2+\ldots\right]}$$

Substituting the expressions for the velocities into the drag equation,

$$D_0=\int_W\sqrt{\frac{2}{\rho_0}\frac{H_0-p_0}{F_0}}-\sqrt{\frac{2}{\rho_1}\frac{H_1-p_1}{F_1}+\frac{2}{\rho_1}\left[(p_1-p_0)+\frac{p_1}{2\gamma}\left(\frac{p_1-p_0}{p_1}\right)^2+\ldots\right]}\times\rho_1\sqrt{\frac{2}{\rho_1}\frac{H_1-p_1}{F_1}}dy_1$$

Now

$$c_{d_0}=\frac{D_0}{c\frac{\rho_0}{2}U_0^2}=\frac{D_0F_0}{c(H_0-p_0)}$$

where c is the airfoil chord.

Finally

$$c_{d_0}=2\int_W\left\{\sqrt{\frac{\rho_1}{\rho_0}}-\frac{\sqrt{\frac{H_1-p_1}{F_1}+\left[(p_1-p_0)+\frac{p_1}{2\gamma}\left(\frac{p_1-p_0}{p_1}\right)^2+\ldots\right]}}{\sqrt{\frac{H_0-p_0}{F_0}}}\right\}\times\sqrt{\frac{H_1-p_1}{H_0-p_0}\frac{F_0}{F_1}}d\left(\frac{y}{c}\right)$$

If the velocities are so low that compressiblity can be neglected, $\rho_0=\rho_1$; $F_0=F_1=1$; and $\frac{p_1}{2\gamma}\left(\frac{p_1-p_0}{p_1}\right)^2$ is negligible compared with p_1-p_0. The drag equation reduces to the form given by Jones

$$c_{d_0}=2\int_W\sqrt{\frac{H_1-p_1}{H_0-p_0}}\left(1-\sqrt{\frac{H_1-p_0}{H_0-p_0}}\right)d\left(\frac{y}{c}\right)$$

REFERENCES

1. Doetsch, H.: Profilwiderstandsmessungen im grossen Windkanal der DVL. Luftfahrtforschung, Bd. 14, Lfg. 4/5, 20. April 1937, S. 173–178.
2. Jacobs, Eastman N., and Sherman, Albert: Airfoil Section Characteristics as Affected by Variations of the Reynolds Number. T. R. No. 586. N. A. C. A., 1937.
3. Jacobs, Eastman N., and Rhode, R. V.: Airfoil Section Characteristics as Applied to the Prediction of Air Forces and Their Distribution on Wings. T. R. No. 631, N. A. C. A., 1938.
4. The Cambridge University Aeronautics Laboratory: The Measurement of Profile Drag by the Pitot-Traverse Method. R. & M. No. 1688, British A. R. C., 1936.
5. Young, A. D., and Maas, J. N.: The Behaviour of a Pitot Tube in a Transverse Total-Pressure Gradient. R. & M. No. 1770, British A. R. C., 1937.
6. Jones, B. Melvill: Flight Experiments on the Boundary Layer. Jour. Aero. Sci., vol. 5, no. 3, Jan. 1938, pp. 81–94.
7. Garrick, I. E.: Determination of the Theoretical Pressure Distribution for Twenty Airfoils. T. R. No. 465, N. A. C. A., 1933.

TABLE I.—SECTION ORDINATES OF THE SMOOTH WING AND THE N. A. C. A. 2414.5 WING. CHORD, 8.86 FEET

[All values in percent chord]

Station	Smooth wing		N. A. C. A. 2414.5	
	Upper	Lower	Upper	Lower
0	0	0		0
1.25	2.45	−2.07	2.63	−1.98
2.5	3.42	−2.84	3.60	−2.75
5	4.75	−3.74	4.92	−3.69
7.5	5.72	−4.33	5.88	−4.30
10	6.43	−4.76	6.64	−4.70
15	7.57	−5.22	7.75	−5.20
20	8.34	−5.39	8.46	−5.42
25	8.83	−5.40	8.92	−5.45
30	9.10	−5.32	9.13	−5.37
40	8.98	−4.90	9.01	−5.01
50	8.32	−4.31	8.35	−4.45
60	7.34	−3.62	7.31	−3.71
70	5.96	−2.87	5.95	−2.90
80	4.25	−2.04	4.30	−2.04
90	2.32	−1.15	2.39	−1.11
95	1.28	−.70	1.31	−.65
100	.12	−.12	(.15)	(−.15)
100				0
			L. E. Rad.. 2.40 Slope of radius through end of chord: 2/20	

TABLE II.—SUMMARY OF PROFILE-DRAG TESTS

Wing lift coefficient, C_L	Reynolds Number, R (millions)	Section profile-drag coefficient. c_{d_0}	Air condition
Smooth Wing			
0.35	10.9	0.0063	Rough.
.295	11.5	.0066	Smooth.
.28	11.7	.0067	Rough.
.25	12.4	.0065	Do.
.25	12.5	.0068	Smooth.
.23	13.0	.0068	Rough.
.22	13.5	.0069	Smooth.
.20	13.9	.0068	Rough.
.19	14.4	.0068	Smooth.
.225	13.1	.0069	Rough.
.185	14.1	.0069	Smooth.
.175	14.9	.0069	Do.
Original Wing			
0.29	11.9	0.0103	Smooth.
.26	12.4	.0101	Do.
.23	13.2	.0101	Do.
.19	14.6	.0103	Do.
.17	14.8	.0100	Do.